

Mode Transitions in an Oscillating Liquid Sheet

A. Lozano*, E. Calvo, J.A. García, and F. Barreras
LITEC, CSIC-Univ. Zaragoza
María de Luna, 10, 50018 Zaragoza, Spain

Abstract

Longitudinal oscillations in air-blasted or air-assisted liquid sheets have been the subject of a large number of papers in the last thirty years. Frequency and sometimes amplitude are the main parameters used to characterize these oscillations. Attending to them, and also in dependence on the surface topology (e.g. presence of perforations or ligaments) different oscillation modes have been described. In most works, two or at most three regimes are considered. Following these previous descriptions, this experimental work has found that some sub-modes can also be discerned. For some liquid and air flow rates up to 6 modes have been observed with defined transitions among them.

Introduction

Over the last few years, the large aspect ratio air-blasted or air-assisted liquid sheet has been extensively studied and has almost become a canonical flow. This is because, in spite of its simplicity, it is very suitable to study the complex mechanisms behind atomization, and in particular, the onset and growth of the instabilities that eventually lead to the liquid break up. Although the first studies on liquid sheets initiated in the 19th century [1], limiting the references only to air-assisted or air-blasted configurations with large aspect ratio, the first reported experimental investigations date from 1980 [2, 3]. A large number of well-known manuscripts, published in the next two decades [4-6], presented mostly phenomenological analysis, with a main interest in predicting the influence of the physical properties on the spray cloud characteristics. More recently, some other experimental works [7-9] have been published, targeting the analysis in the region close to the nozzle exit. It has been demonstrated that it is in this region where instabilities develop and grow, causing liquid sheet oscillations of increasing amplitude and eventually, the break-up. A complete review of the numerical approach can be found in Sirignano and Mehring [10]. Dumouchel also includes the liquid sheet atomization in a very recent review paper [11].

The characteristics of the sheet longitudinal oscillations have been the subject of a large number of papers. The topic has been covered both experimental and numerically. As usual, frequency, and occasionally, amplitude have been the main parameters analyzed to characterize these oscillations. In some studies, the frequency has been related to the sheet visual aspect to define different oscillation modes. For example, Stapper and Samuelsen [5] describe a “cellular” break up mode opposed to a “streamwise ligament” one, depending on the presence of either a mesh of perforations, or longitudinal ligaments. Similarly, Mansour and Chigier [4,6] define three zones A, B and C dependent on the gas-liquid relative velocity. According to their description, zone B is characterized by a single dominant sinusoidal mode, and the break up occurs after the appearance of streamwise ligaments, while in zone C the presence of dilatational waves are claimed to prevent the dominant growth of the sinusoidal ones. In zone A, for low water velocities, the break up in longitudinal filaments occurs right at the nozzle lip and no intact sheet length is visible, preventing its accurate experimental measurement.

In this work, the longitudinal oscillation of a gas co-flowing liquid sheet has been examined, trying to identify different modes attending to sudden variations in frequency or spray angle. As will be seen, these changes can imply angle and frequency increases or reductions, or coexistence of more than a single dominant oscillation wave.

Materials and Methods

The facility in which the present measurements have been obtained has been described in detail in previous papers [8, 9, 12]. For this reason, only the most important characteristics, relevant to the results that will be shown, will be presented here. Water injected at the top of the nozzle head exits vertically forming a sheet with a span of 80 mm and a width of 0.4 mm. The sheet is surrounded by two air streams that flow in parallel to both sides of the liquid curtain with an exit width of 3.45 mm each. Water volumetric flow rate has extended up to 640 l/h, corresponding to a maximum liquid velocity U_w of 5.55 m/s. The maximum air flow velocity has been measured to be $U_a = 70$ m/s. The measurements obtained in the present experiments are in very good agreement with those previously acquired in the same facility [9, 12]

* Corresponding author: alozano@litech.csic.es

To determine the oscillation frequency, the acoustic signal has been detected using a type 2669 Brüel & Kjaer pressure transducer. The Fast Fourier Transform (FFT) of the periodic signal has been obtained in a Tektronix TDS3012 oscilloscope equipped with a TDS3FFT module. Image sequences have also been recorded with a 512x512 CMOS RedLake HS-4 high-speed camera.

Results and Discussion

While measuring the oscillation frequency for different air and water velocities, several oscillation modes have been detected, with some particular characteristics. In general, the procedure to locate them has consisted in fixing the air velocity, and then sweeping over the full range of water velocities. It is to be noted that hysteresis has been observed in these cycles, so that the transition points between modes have been found to be slightly different when water velocity was being either increased or decreased.

Oscillation modes

Although sometimes it has been difficult to clearly separate between different modes, the following classification is proposed to explain the present measurements and observations, corresponding to increasing water flow rates:

- Mode 0 (M0): similar to Mansour and Chigier zone A. Includes the situation where the low water flow rate is not enough to form a continuous sheet and exits from the nozzle as discrete filaments, and the initial stage of an incipient sheet. These two situations could be considered as sub-modes. The frequency spectra of the acoustic microphone signal present a peak at low frequencies, that seems to be nearly independent of U_a .
- Mode 1 (M1): there is already a visible sheet that oscillates with two coupled frequencies. The presence of the two waves can be discerned by eye. The highest frequency, which is identified as a small ripple on the sheet surface is a multiple of the principal oscillation frequency.
- Mode 2 (M2): The spray angle increases, the harmonic peaks disappear and only a single dominant frequency of sinusoidal oscillation remains. For low air velocities ($U_a < 24$ m/s), this mode can be divided into two sub-zones, M2a and M2b, with a transition between them. For M2b, which takes place for higher water flow rates, the spray angle is narrower, and the oscillation frequency is lower. In each one of the sub-modes, both frequency and spray angle are relatively stable.
- Mode 3 (M3): single dominant sinusoidal oscillation after a sudden reduction in spray angle and an increase in frequency.
- Mode 4 (M4): further reduction of the angle, with de-phasing in the sheet edges oscillation. The edges tend to approximate to each other at the sheet far end. A new peak appears in the FFT spectrum, coexisting with the dominant peak of mode 3, although both of them are lower than in the previous zone. This mode is only evident for air velocities over 22.5 m/s. For lower velocities, mode 3 transitions directly to mode 5 below. This mode could already be included in Mansour and Chigier Zone C, which extends also to Mode 5.
- Mode 5 (M5): No oscillation frequency can be measured any longer. For large air velocities this mode cannot be reached even for the maximum water flow rates.

Mode transitions

Transitions between consecutive modes are detected attending to spray angle variations (by visual observation), or analyzing the FFT spectra of the acoustic signal. Each one of these transitions presents specific particularities:

- Transition 0 (T0): between modes M0 and M1. Mode M0 is characterized by a low frequency peak, while the peak in mode M1 corresponds to a higher frequency. Transition T1 is assigned to the point where both peaks have approximately the same height.
- Transition 1 (T1): between modes M1 and M2. It is difficult to assess unambiguously. In these experiments, it has been determined combining visual observations, high speed recordings, and peak displacements in the FFT spectra. This transition presents hysteresis, occurring at different values if the flow rates are increasing or decreasing. In general, it seems that when the flow moves from mode M1 to M2, the number of large droplets in the spray periphery decreases.
- Transition 2a (T2a): between modes M2a and M2b. Detected initially in a coarse manner by a visual change in the spray angle. The exact point can be more precisely determined examining the appearance of a lower frequency peak in the FFT spectrum of the microphone signals. This transition is only detected for $U_a < 24$ m/s.
- Transition 2 (T2): between modes M2 and M3. Initial detection associated to a reduction in the spray angle, more accurately evidenced by an abrupt change in the oscillation frequency, displaced towards higher values. This transition has been observed for all the range of air velocities. In mode M2 large droplets in the outer part of the spray can be discerned. In mode M3 the large peripheral droplets disappear, and the spray looks more uniform.

- Transition 3 (T3): between modes M3 and M4 for $U_a > 22.5$ m/s (otherwise, the transition is to M5 directly). Difficult to be determined visually. Associated to the appearance of a second peak in the frequency spectrum. The transition is assigned to the moment when both peaks have similar heights.
- Transition 4 (T4): the entrance in mode M5 is associated to the disappearance of a dominant peak in the FFT spectrum.

Water velocities for which transitions between consecutive modes occur, for different air velocities, are plotted in Fig. 1.

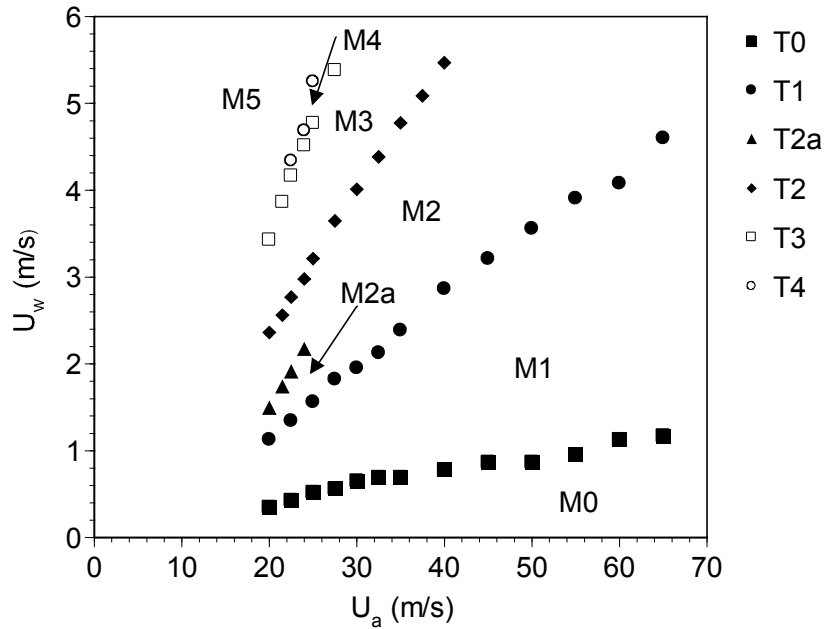


Figure 1. Map of the different mode transitions

Example

As an example, the oscillation for a fixed air flow velocity of 25 m/s will be analyzed in more detail. Frequency measurements are presented in Fig. 2. The points where a transition has been visually observed are enclosed in a circle.

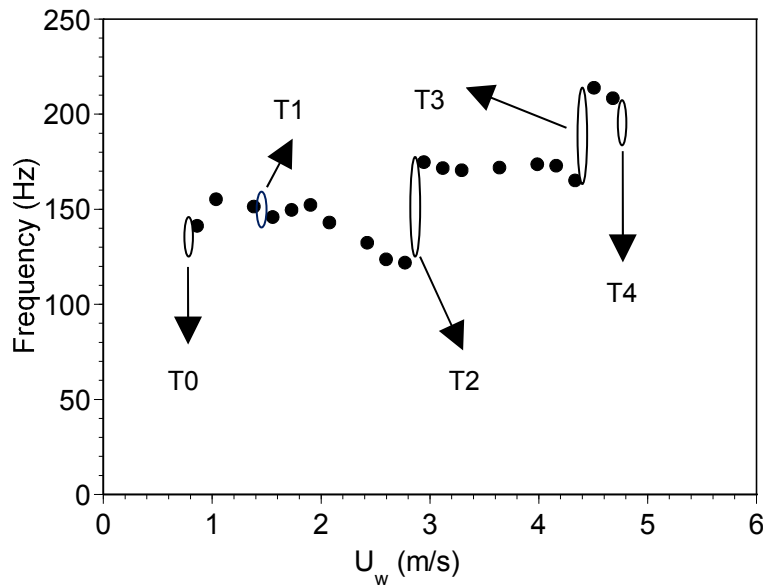


Figure 2. Oscillation frequency values vs. water velocity for an air velocity of 25 m/s. Regions where a mode transition has been observed are enclosed in a circle

Images of the oscillating sheet before and after transition T1, together with the corresponding frequency spectra are displayed in Fig. 3. To our knowledge, this is the first time that this transition, difficult to be discerned by frequency measurements, but clearly noticeable from visual analysis, is reported. In this case, the increase in water velocity results in a slight decrease in the oscillation frequency, and an enlargement of the spray angle. A notorious elongation of the wavelength is also visible in the image. Looking at the figure, it can be concluded that at $U_w = 1.3$ m/s there is a superposition of two different frequencies, the second one, multiple of the first, completely disappearing when U_w reaches 1.5 m/s. For these liquid velocity values, the corresponding momentum flux ratio (MFR), defined as $(\rho_a U_a^2)/(\rho_w U_w^2)$ ranges from 0.53 to 0.4.

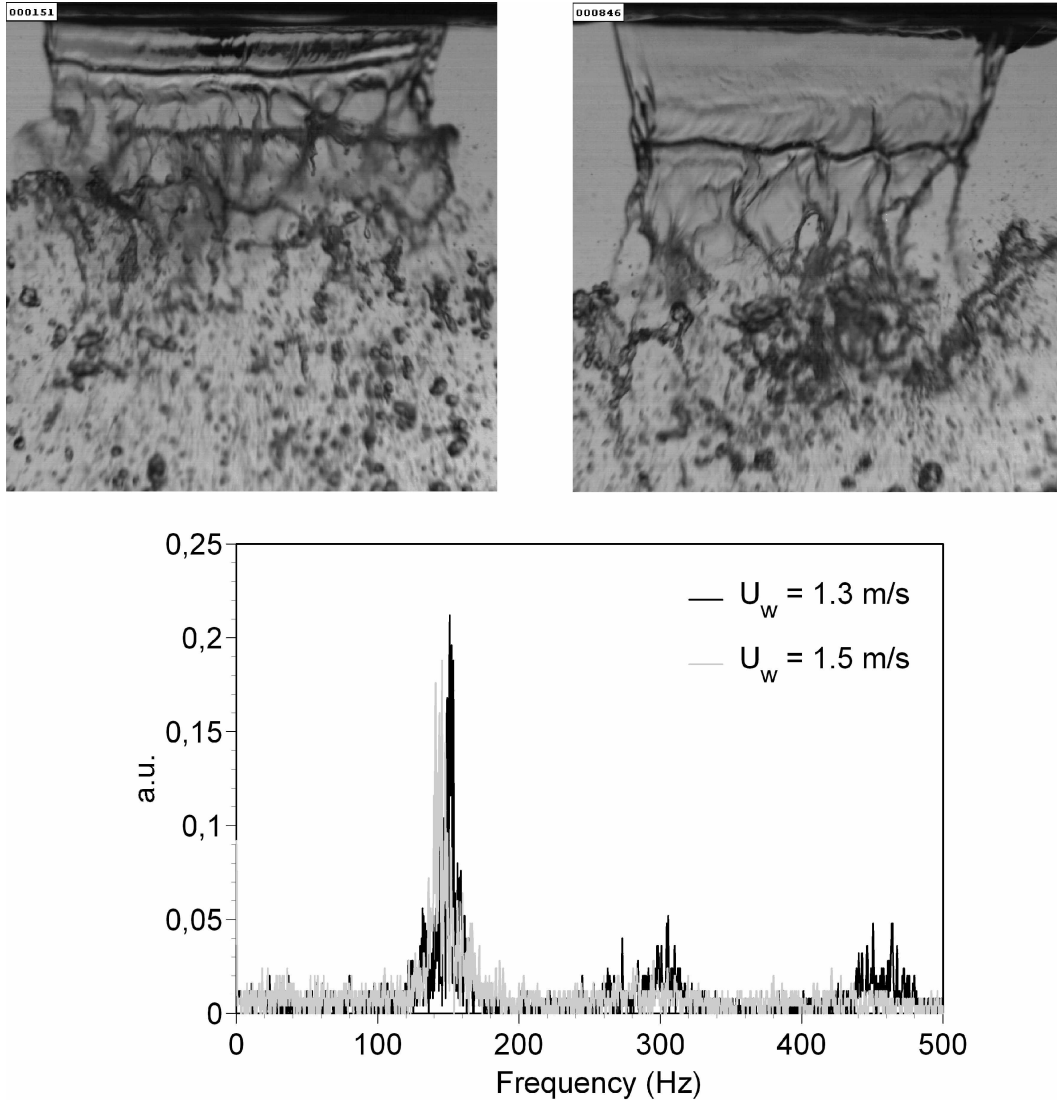


Figure 3. Transition observed when U_w increases from 1.3 m/s (left) to 1.5 m/s (right). $U_a = 25$ m/s

The third observed transition T2 is displayed in Fig. 4. Corresponds to an increase in water velocity from 2.7 m/s to 2.9 m/s (MFR decreasing from 0.12 to 0.11), and is reflected as a discontinuous increase in the oscillation frequency, that is accompanied by a reduction in the spray angle. The physical aspect of the sheet is similar in both images, but the wavelength seems to be longer after the transition.

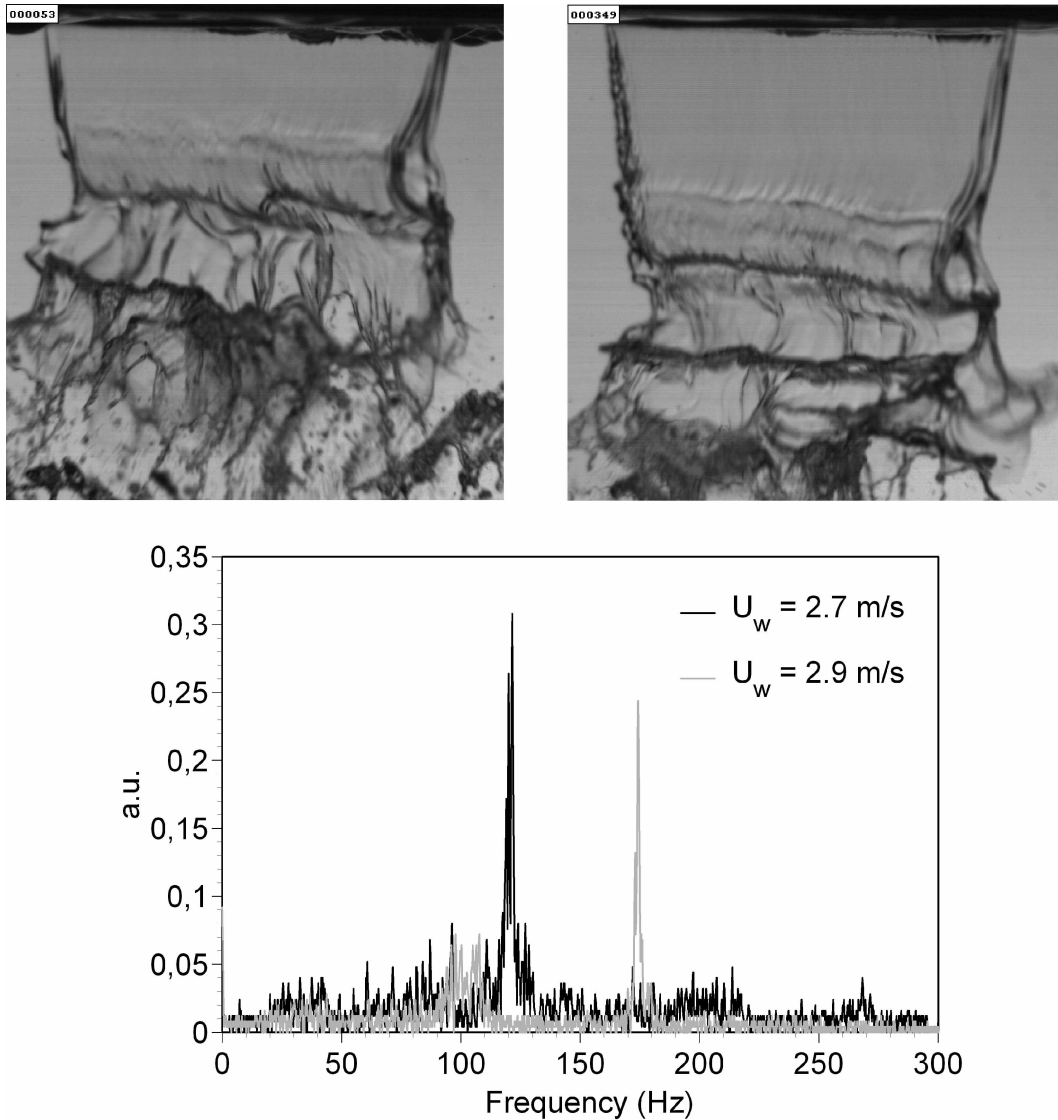


Figure 4. Transition observed when U_w increases from 2.7 m/s (left) to 2.9 m/s (right). $U_a = 25$ m/s

Finally, transition T3, detected as water velocity increases from 4.15 m/s to 4.3 m/s (MFR decreasing from 0.052 to 0.048), can be discerned from the photos and plots displayed in Fig. 5. In this case, the effect is manifested as an increase in the oscillation frequency and a sudden decrease in the spray angle. For water velocities higher than 5.0 m/s the atomization is poor, and the frequency measurements are inaccurate. This point would be identified as the transition to mode M5, where clear peaks are no longer visible in the frequency spectrum.

Analyzing all these transitions, it can be concluded that they are of different nature. Location of T0 and especially T1 might be associated to resonances of the experimental facility, and are probably influenced by some imperfections in the nozzle lips, particularly some misalignment in the parallelism between both of them. On the other hand, T3 and T4 appear to be related to sheet edge effects. In particular, we believe that T3 corresponds to the change from zone B to C as defined by Mansour and Chigier. For water velocities over 4.5 m/s, the sheet edges do not remain parallel down to the break up distance, but they approach each other, tending to collapse as occurs when no air flow is present.

It is also interesting to note that in T1, the oscillation frequency slightly decreases while the wavelength is enlarged, but in T2 there appears to be a simultaneous increase in both frequency and wavelength and in T4 the frequency increases while the wavelength seems to shrink. In the T2 case the wave propagation velocity has to increase, due to the acceleration of the water stream in its interaction with the air. However, in the first case, the wave propagation velocity might remain constant.

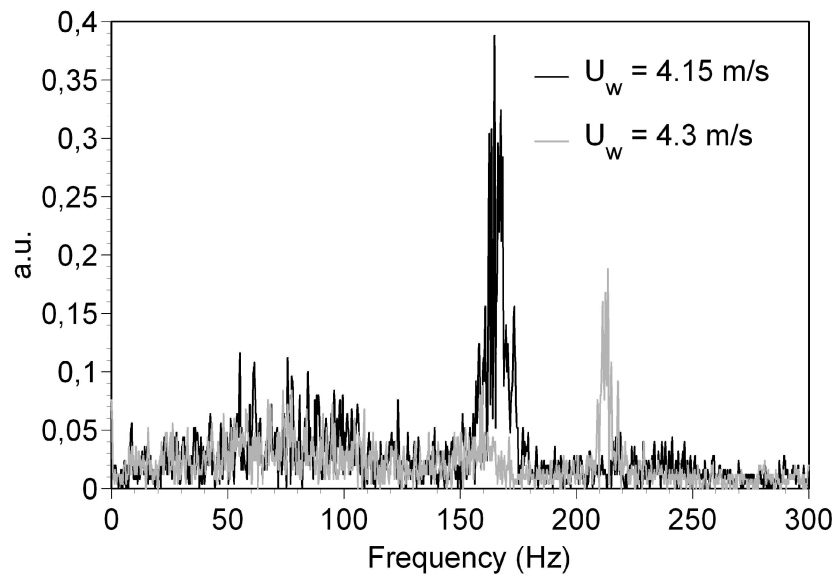
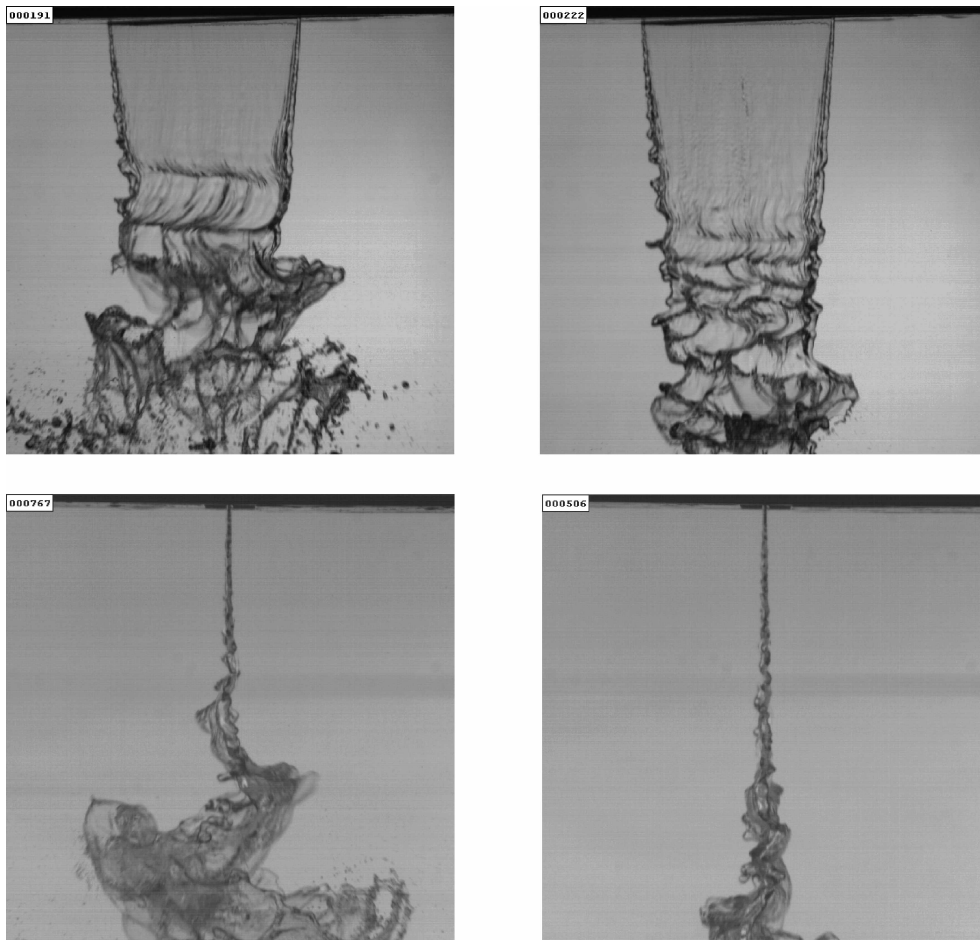


Figure 5. Transition observed when U_w increases from 4.15 m/s (left) to 4.3 m/s (right). $U_a = 25$ m/s

Nomenclature

U velocity [$\text{m}\cdot\text{s}^{-1}$]
 ρ density [$\text{kg}\cdot\text{m}^{-3}$]

Subscripts

a air
 w water

References

- [1] Savart, F., Memoire sur le choc d'une veine liquide lancée contre un plan circulaire, *Ann. de chim.* vol. 54, 56-87 (1833).
- [2] Rizk, N.K., and Lefebvre, A.H., The Influence of Liquid Film Thickness on Airblast Atomization, *J. Eng. Power*, vol. 102, 706-710 (1980)
- [3] Arai, T. and Hashimoto, H., Disintegration of a Thin Liquid Sheet in a Concurrent Gas Stream, *6th Intl. Conf. on Liquid Atomization and Spray Systems*, London, UK, July 1985.
- [4] Mansour, A. and Chigier, N., Disintegration of Liquid Sheets, *Phys. Fluids A*, vol. 2,(5), 706-719, (1990).
- [5] Stapper, B. E., Samuelsen, G. S., An Experimental Study of the Breakup of a Two-dimensional Liquid Sheet in the presence of co-flow air shear, *AIAA Paper # 90-0461*, (1990).
- [6] Mansour, A. and Chigier, N., (1991), Dynamic Behavior of Liquid Sheets, *Phys. Fluids A*, vol. 3,(12), 2971-2980, (1991).
- [7] Vich, G., Dumouchel, C., Ledoux, M., Mechanisms of Disintegration of Flat Liquid Sheets, *12th Ann. Conf. ILASS-Europe*, Lund, Sweden, June19-21 (1996).
- [8] Lozano, A. Barreras, F., Hauke, G., and Dopazo, C., On the Longitudinal Perturbation of an Air-Blasted Liquid Sheet, *J. of Fluid Mech.*, vol. 437, 143-173 (2001).
- [9] Lozano, A. Barreras, F., Experimental Study of the gas flow in an Air-blasted Liquid Sheet, *Exp. in Fluids*, vol. 31 (4), 367-376 (2001)
- [10] Sirignano, W.A., and Mehring, C., Review of theory of distortion and disintegration of liquid streams, *Prog. Energy and Comb. Science*, vol. 26, 609-655 (2000).
- [11] Dumouchel, C., On the experimental investigation on primary atomization of liquid streams, *Exp. in Fluids*, vol. 45 (3), 371-422, (2008).
- [12] Lozano, A., Barreras, F., Siegler, C., Löw, D., The effects of sheet thickness on the oscillation of an air-blasted liquid sheet, *Exp. in Fluids*, vol. 39 (1), 127-139, (2005).